Library

N72-30245

DRA

TECHNICAL REPORT HSM-R5-72
MAY 24, 1972

AERONAUTICAL NOISE SUPPRESSION AT TRANSONIC MACH NUMBERS

FINAL REPORT
CONTRACT NO. NAS8-27503

HUNTSVILLE DIVISION CHRYSLER CORPORATION

TECHNICAL REPORT R5-72

NAS8-27503

AERONAUTICAL NOISE SUPPRESSION

AT TRANSONIC MACH NUMBERS

By

George F. McCanless, Jr.

May 24, 1972

FOREWORD

This report was prepared by the Engineering Mechanics Department, Huntsville Division, Chrysler Corporation. The work was authorized by NASA Contract NAS 8-27503 which was issued by the Unsteady Gasdynamics Branch, Aerophysics Division, Aero-Astrodynamics Laboratory, Marshall Space Flight Center, Huntsville, Alabama. The study was conducted to obtain a higher quality of dynamic design data describing the unsteady aerodynamic environment of bodies traveling through the atmosphere. Generally, models instrumented with acoustic pressure transducers are placed in wind tunnels to generate this dynamic environmental data and these transducers sense the fluctuating pressures generated by the flow of air over the models. However, the background noise of the wind tunnel is also sensed and the disturbances degrade the acoustic test data. The study was directed toward the following four specific objectives: (1) The phenomena of noise generation in this facility and in other transonic wind tunnels was analyzed, (2) The feasibility of conducting acoustic test in impulse facilities was considered, (3) The amplitude and frequency characteristics of noise in the MSFC 0.80 m High Reynolds Number Ludwig Tube were investigated, and (4) Methods of reducing the noise were established.

ABSTRACT

Tests measuring wind tunnel background pressure fluctuations were conducted in the MSFC 0.80 m High Reynolds Number Ludwig Tube. The tests were conducted so that improved unsteady aerodynamic data will be provided for the design of aeronautical vehicles. The wind tunnel model and instrumentation were fabricated by MSFC personnel and preliminary data reduction was performed by Chrysler personnel. This report describes the preliminary results of the facility calibration. The noise generation mechanisms are discussed. The ability of conducting short duration acoustic tests is demonstrated, and amplitude and frequency data are given. Techniques of noise reduction are included.

TABLE OF CONTENTS

LIST OF FIGURES

1.0 INTRODUCTION

Background noise exists in test sections of transonic wind tunnels and these disturbances interfere with unsteady aerodynamic tests. Because air flows tend to become unstable just below the speed of sound, transonic buffeting pressures are generated that impose dynamic loads on the structures of aeronautical vehicles. Thus, unsteady aerodynamic data from transonic wind tunnels is required to assure the structural integrity of vehicles. To obtain valid buffeting design data, two types of tests are conducted. One utilizes rigid models instrumented with acoustic pressure transducers, whereas the other incorporates flexible models whose aeroelastic deflections are measured.

Unfortunately, transonic wind tunnels contain high level background pressure fluctuations which are sensed by the models and thus degrade the test results. To determine the nature of these disturbances so that the problem can be mitigated, numerous investigators have conducted acoustic calibrations in transonic wind tunnels throughout the world. The calibrations have indicated that, in general, the background noise consists of high-level narrow-band oscillations that are superimposed on low-level broad-band oscillations. The narrow-band oscillations are strong disturbances which concentrate near discrete frequencies. The broad-band oscillations are weak disturbances which occur over continuous spectrums of frequencies. The investigations have shown that the amplitude of the background noise is generally within the range of the transonic buffeting data which is the objective of unsteady aerodynamic tests. In the center of test sections, the fluctuation pressure coefficients range from $\Delta C_p = 0.9\%$ to $\Delta C_p = 5.5\%$. The amplitudes of the required measurements vary from $\Delta C_p = 0.5\%$ under a turbulent boundary layer of a body to $\Delta C_p = 10.0\%$ under an oscillating shock wave. Thus, the background noise levels in the test sections must be reduced so that the necessary acoustic data can be obtained.

The calibrations have shown that a significant portion of the noise is caused by air flowing over porous walls or slotted walls as shown in Figure 1. These types of walls compensate for the model-occupied space in the test sections by passing air between the test sections and the surrounding plenum chambers.

Porous-wall test sections contain numerous holes in the walls and they act as whistles by generating porous-wall edgetones. Ten years before the first practical transonic wind tunnels were built, Brown[1, 2, 3 & 4] conducted studies of classical edgetones. They were found to occur in four distinct frequency stages and criteria for their occurrence were established. The wind tunnel calibrations reveal that the edgetone mechanism causes porous-wall oscillations to occur also in four distinct narrow-band frequency stages. The porous-wall edgetones found in wind tunnels are related to the classical edgetones.

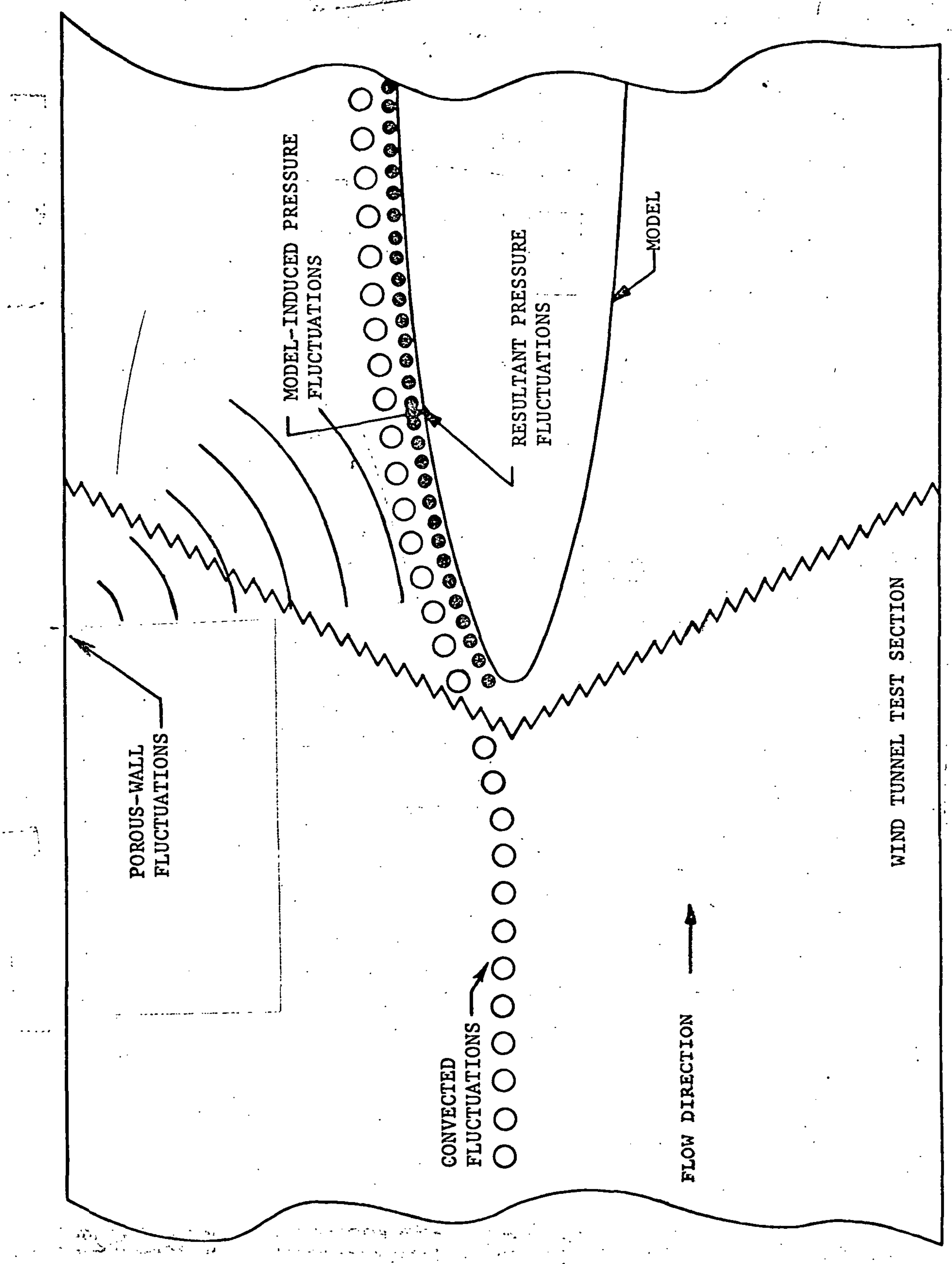

Figure 1. Wind Tunnel Noise

The slotted-wall test sections utilize open slots that traverse the walls in the direction of flow. The open slots generate noise by the same mechanism that rocket exhaust jets generate noise. The shearing between the air in the test sections and air in the plenum chambers creates large eddies that cause pressure fluctuations.

In both porous and slotted-wall test sections, pressure surges in the plenum chambers have been observed to generate test section noise. In addition, turbulent boundary layers on the solid portions of test sections generate disturbances.

Externally generated noise has been observed to be transmitted to the test sections both through the air and through structures. Control valve jets have been found to be external noise sources in blowdown wind tunnels and compressor blade fluctuations have been established as a noise source in continuous facilities. Unstable flow in the diffuser of both types can reach the test sections.

This report describes the acoustic calibration of the MSFC 0.80 m High Reynolds Number Ludwig Tube. This facility is potentially very quiet since it does not utilize a control valve or a continuous compressor. To obtain calibration data, acoustic transducers were mounted on a ten-degree included angle cone which was placed in the center of the test section. A transducer was also placed on the wall of the test section. The data was processed by a multiplex system and recorded on magnetic tape. Preliminary data reduction was carried out with a correlator. A boundary layer rake was mounted on the wall at the rear of the test section. To establish the significant factors that govern the noise generation, parametric variations were made in Mach Number, stagnation pressure, and porosity. Each of these was found to influence the disturbances.

2.0 FLOW MODEL OF POROUS-WALL EDGETONES

Various acoustic calibrations of porous-wall transonic wind tunnels have shown the existence of strong narrow-band pressure fluctuations. Caused by the flow of air over holes in the walls, the frequencies of these porous-wall edgetones occur in four discrete stages which are similar to harmonics. The porous-wall edgetones are related to the classical edgetones shown in Figure 2.

A hypothetical flow model is developed here which is consistent with experimental results from the seven wind tunnels described in Reference 5 as well as with data obtained from the MSFC 0.80 m High Reynolds Number Ludwig Tube. The model yields the following frequency equation:

$$(f \ell / u_\infty) = (j-0.5)(u_V/u_\infty)(1-0.36\, u_\infty / c) \qquad (1)$$

Where c is the speed of sound at the free stream stagnation conditions in m/sec; f is the edgetone frequency in Hz; j is the stage parameter of 1, 2, 3, or 4; ℓ is the resonant separation distance in m (i.e. the distance from the front to the rear of the holes, minus 1.4×10^{-3}m); u_∞ is the free stream velocity of the wind tunnel test sections in m/sec; and u_V is the convective velocity of the vortices in m/sec. The ratio of the vortex velocity to free stream velocity, u_V/u_∞, is determined as 0.220, 0.235, 0.250, and 0.265 respectively for stage 1, 2, 3, and 4 edgetones. Eq. (1) is used in the last section of this report to normalize the frequency data from seven porous-wall wind tunnels and from the Ludwig tube.

The flow model for the incompressible case is shown on Figure 3. It is based on the edgetone studies of Brown[1, 2, 3, & 4] and Curle[6] as well as on the wind tunnel acoustic calibrations. The model is a hypothetical explanation of the mechanism of noise generation in porous-wall facilities; the determination of the actual porous-wall edgetone phenomena must await detailed experimental studies of the flow patterns. In the model, vortices or regions of concentrated vorticity, are assumed to form just downstream from the leading edges of the holes. Vortices are frequently observed to be generated by flow separations at corners; the vortices at the edges of canoe paddles being familiar examples of this phenomenon. At porous walls they form 1.4×10^{-3} m downstream from the leading edges. The resonant separation length, ℓ, is the distance from these points to the aft edges of the holes. As the vortices pass over the aft edges they are significantly strengthened. The circulation from these strengthened vortices is in the clockwise direction and it tends to move the stream away from the upstream edges of the holes. For incompressible flow this circulation is communicated upstream in a very short period of time compared with the time required for other events. The movement of the stream away from the upstream corner tends to retard the formation of vortices. Thus vortices form 1.4×10^{-3} m downstream from the leading edges when two vortices straddle the downstream edges and the nodal points which lie halfway between the vortices are located at the downstream edges.

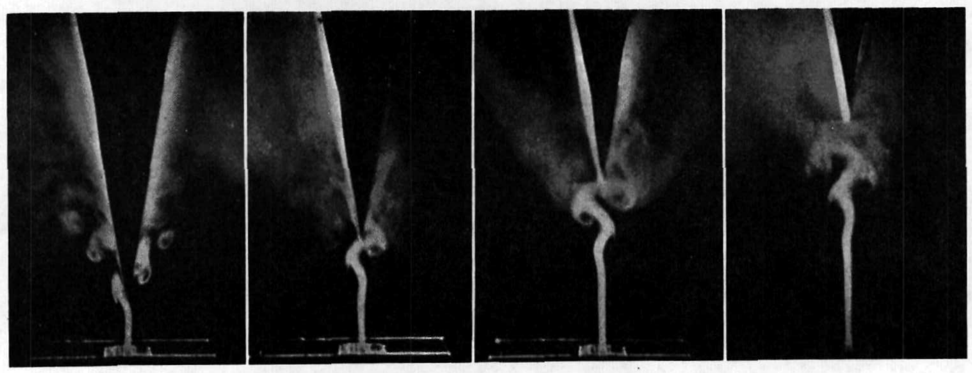

Figure 2. Brown's Edgetone Studies

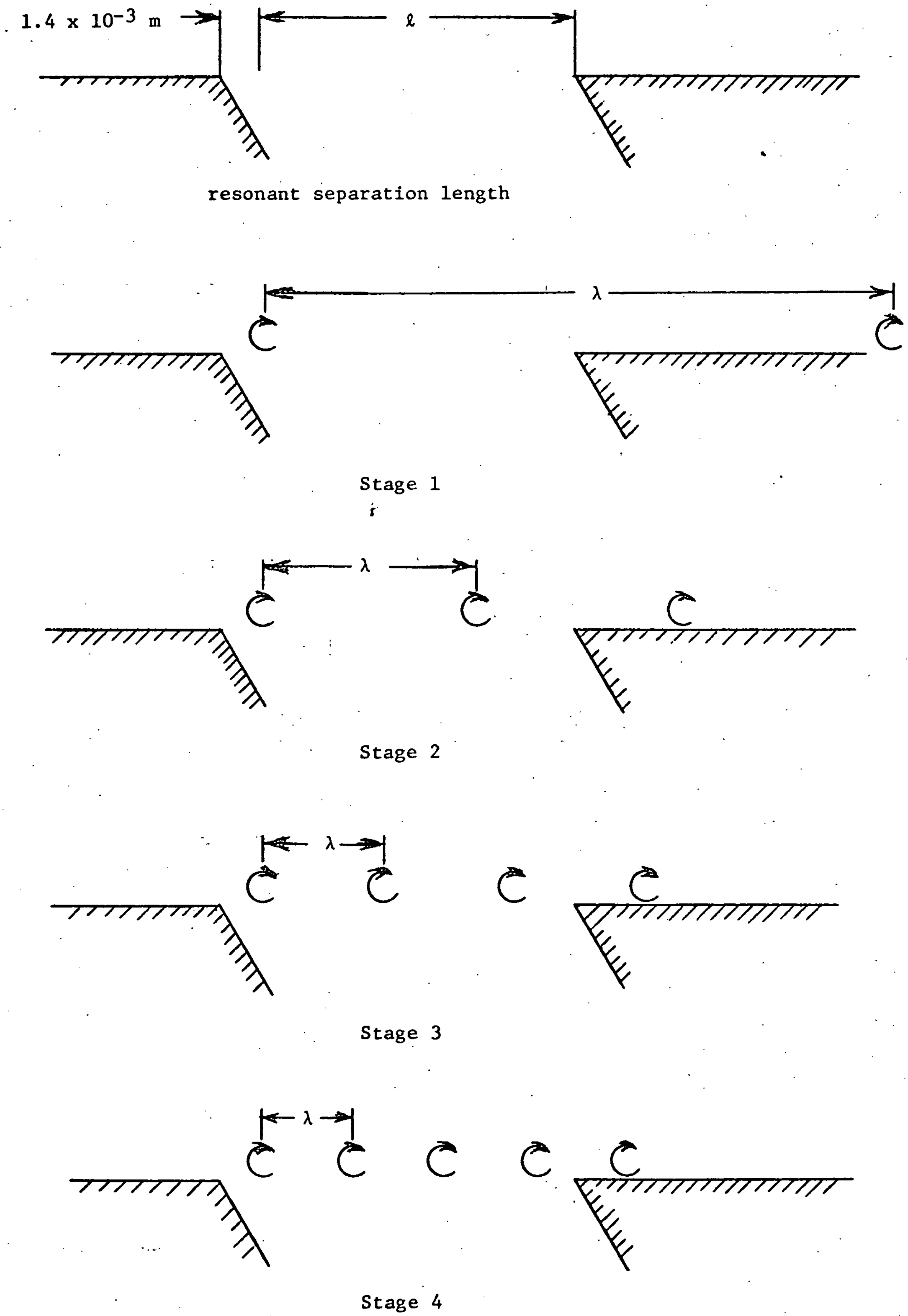

Figure 3. Flow Model of Porous-Wall Edgetones

The frequencies of the pressure fluctuations, which are the frequencies of vortex generation, f, are given by dividing the wave lengths between the vortices, λ, into the vortex convective velocities, u_V. In nondimensional form this is:

$$(f \ell / u_\infty) = (\ell / \lambda)(u_V / u_\infty) \quad (2)$$

Figure 3 shows that the resonant separation distance is related to wave length by $\ell = (j-0.5)\lambda$ which transforms the incompressible frequency equation to:

$$(f \ell / u_\infty) = (j-0.5)(u_V / u_\infty) \quad (3)$$

This equation and Eq. (1) yield the same results for small values of the free stream velocity with respect to the speed of sound.

For compressible flow the time required for the vortex circulation to be transmitted upstream from the rear edges of the holes to the point of vortex formation is given by $\Delta t = \ell / (c-u_e)$. Here c is the speed of sound at the stagnation conditions of the free stream and u_e is the "effective" velocity of the shear layer. During the time lapse for the communication of the vorticity upstream the nodes between vortices move downstream a distance $u_V \ \Delta t$. Thus in compressible flow the relation between resonant separation length and wave length is:

$$\ell + u_V \ell / (c-u_e) = (j-0.5)\lambda \quad (4)$$

The data from the acoustic calibrations of the wind tunnels indicate that the ratio of the "effective" velocity of the shear layer to the free stream velocity, u_e/u_∞, is equal to 0.36 for all four stages. Eq. (4) is simplified by observing that the difference between this value and those of the ratios of the vortex velocities with respect to the free stream velocities, u_V/u_∞, is small compared with one. Substituting the simplified form of Eq. (4) into Eq. (2) yields Eq. (1) as the frequency equation of the porous-wall edgetone stages in compressible flow. The wind tunnel data yield values of the ratio of the vortex velocity to free stream velocity, u_V/u_∞, of 0.220, 0.235, 0.250, and 0.265 respectively for stage 1, 2, 3, and 4 edgetones. These values are also consistent with Brown's results. He found that the ratio of the jet vortex velocities to the mean jet velocities ranged from 0.220 to 0.470. Generally the low-stage, large-wave-length cases gave low values of this ratio; whereas, the high-stage, small-wave-length cases yielded the higher values.

3.0 MSFC 0.80 M HIGH REYNOLDS NUMBER LUDWIG TUBE

3.1 FACILITY DESCRIPTION

The MSFC 0.80 m High Reynolds Number Ludwig Tube is basically a high-density, impulse wind tunnel. The supply tube has an inside diameter of 1.32 m and is 119 m long. Coupled to the down stream end of the supply tube is a stilling chamber that has an inlet half-angle of 4 degrees and a maximum diameter of 0.725 m.

The tunnel is equipped with four interchangeable axisymetric nozzles and two interchangeable test sections. This combination provides a Mach Number coverage from M = 0.25 to 2.00. Both test sections are 0.80 m inside diameter. The porous wall transonic test section, which is 2.54 m long, is shown in Figure 4. Variations in porosity are provided by sliding the two concentric porous wall cylinders with respect to one another.

Downstream of the test section is the model support section. The sting pod is supported by two vertical struts which permit a pitch range of ± 18 degrees, while maintaining a fixed center of rotation of the model in the test section. Following the model support section is the diaphragm section. This section provides for the support, clamping, and rupturing of the multi-layer 1.22 m diameter mylar diaphragm.

The components downstream of the diaphragm section are a spool piece, a telescoping diffuser, and a receiver sphere. After each shot, the air exhausts into the receiver sphere and is bleed through a muffler to the atmosphere. At maximum operating pressure of 3.70×10^6 N/m^2 about five shots per day can be made. Air is supplied by the center-wide 18.5×10^6 N/m^2 high pressure air system.

Standard data acquisition is accomplished by a solid state digital data system. The 12 channel system stores the data in memory which can be read out by a card punch. Data is also recorded on a 14 channel magnetic tape system that is read out on a 32 channel direct recording oscillograph.

3.2 TEST SCHEDULE

The schedule of the test is shown in Figure 5. The test schedule was arranged so that the facility operating personnel could run the test program as quickly and economically as possible. The variable operating parameters of the tests comprised Mach Number, stagnation pressure, and porosity. To generate variations in boundary layer thickness, two spoiler rings were placed just upstream of the test section during some of the shots. The influence of the porous-wall holes was investigated by progressively sealing them with tape from the rear of the test section. Comparative data concerning the influence of the holes was also obtained by conducting tests with the solid-wall test section replacing the porous-wall unit.

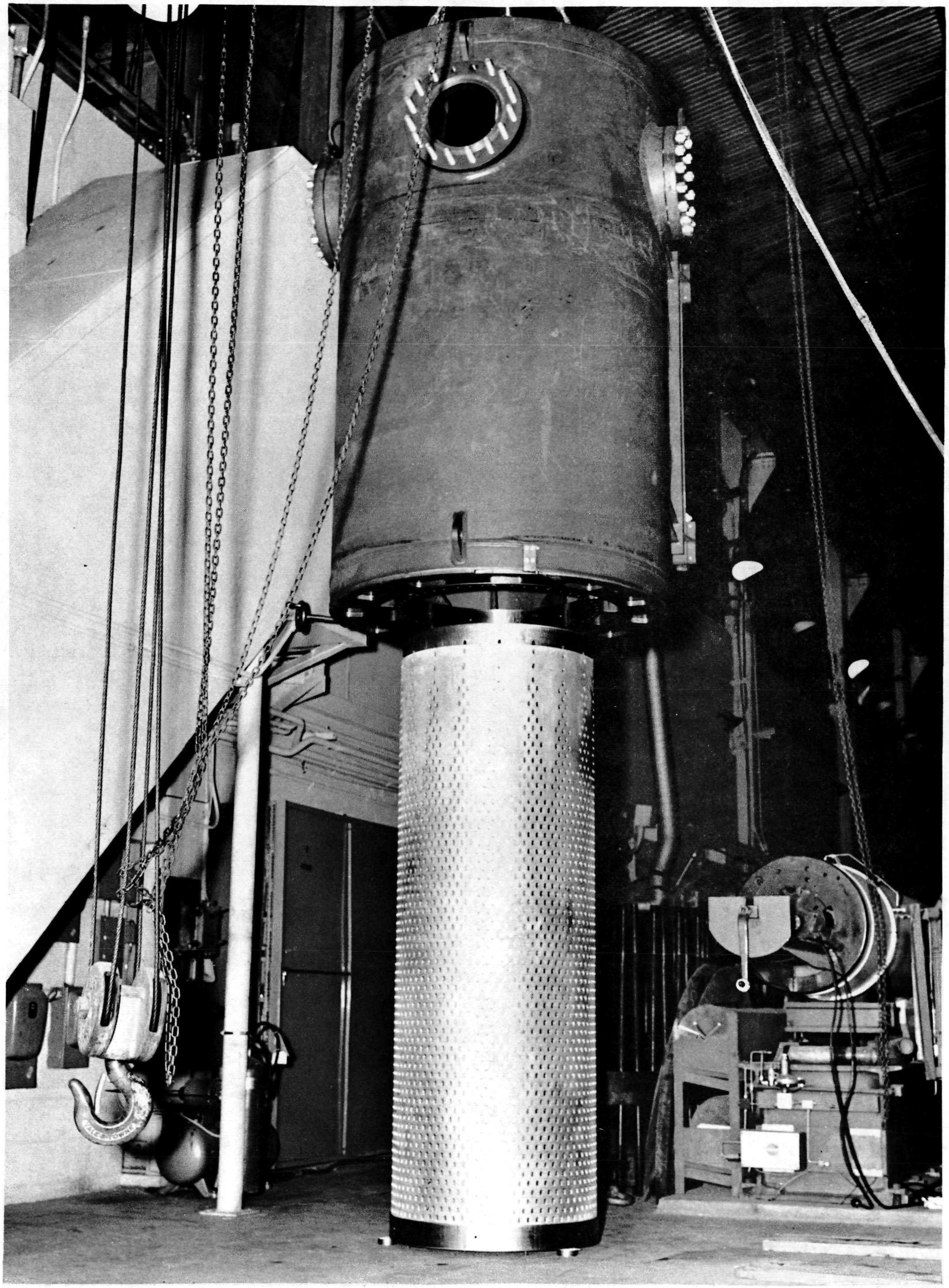

Figure 4. Porous Wall of the High Reynolds No. Ludwig Tube

RUN	NOTE	MACH NO.	POROSITY	$P_o \times 10^{-3}$ (N/m^2)	EFFECT OF
1	a	0.80	1.5	1,400	Mach No. at med P_o
2	a	0.80	1.5	341	Mach No. at low P_o
3		0.70	1.5	341	Mach No. at low P_o
4		0.90	1.5	341	Mach No. at low P_o
5		1.00	1.5	341	Mach No. at low P_o
6		1.40	1.5	341	Mach No. at low P_o
7	r	0.80	1.5	341	Mach No. at low P_o
8	b	0.80	1.5	341	Mach No. at low P_o
9	c	0.80	0.0(1/6 taped)	341	Mach No. at low P_o
10		0.80	0.0(1/3 taped)	341	b.1. Thickness
11		0.80	0.0(1/2 taped)	341	b.1. Thickness
12		0.80	0.0(2/3 taped)	341	b.1. Thickness
13		0.80	0.0(5/6 taped)	341	b.1. Thickness
14		0.80	0.0(all taped)	341	b.1. Thickness
15		0.80	1.5	341	b.1. Thickness
16	d	0.80	1.5	341	b.1. Thickness
17	d	0.80	1.5	1,400	b.1. Thickness
18	d	0.80	1.5	3,700	b.1. Thickness
19	e	0.80	1.5	3,700	b.1. Thickness
20	e	0.80	1.5	341	b.1. Thickness
21	e	0.80	1.5	1,400	b.1. Thickness
22		0.70	1.5	1,400	Mach No. at med P_o
23		0.75	1.5	1,400	Mach No. at med P_o
24		0.85	1.5	1,400	Mach No. at med P_o
25		0.90	1.5	1,400	Mach No. at med P_o
26		0.95	1.5	1,400	Mach No. at med P_o
27		1.00	1.5	1,400	Mach No. at med P_o
28		1.40	1.5	1,400	Mach No. at med P_o
29	r	0.80	1.5	1,400	Mach No. at med P_o
30	b	0.80	1.5	1,400	Mach No. at med P_o
31	c	0.80	1.5	1,400	Mach No. at med P_o
32		0.80	1.5	670	P_o at Mach No. 0.80
33		0.80	0.0	1,400	Por. at Mach No. 0.80
34		0.80	0.75	1,400	Por. at Mach No. 0.80
35		0.80	3.0	1,400	Por. at Mach No. 0.80

Figure 5. Calibration Test Schedule

RUN	NOTE	MACH NO.	POROSITY	$P_o \times 10^{-3}$ (N/m^2)	EFFECT OF
36		0.80	6.0	1,400	Por. at Mach 0.80
37		0.80	10.0	1,400	Por. at Mach 0.80
38		0.70	1.5	3,700	Mach No. at high P_o
39		0.90	1.5	3,700	Mach No. at high P_o
40		1.00	1.5	3,700	Mach No. at high P_o
41		1.20	1.5	3,700	Mach No. at high P_o
42		1.40	1.5	3,700	Mach No. at high P_o
43		0.80	1.5	3,700	Mach No. at high P_o
44	b	0.80	1.5	3,700	Mach No. at high P_o
45	c	0.80	1.5	3,700	Mach No. at high P_o
46		0.80	1.5	3,100	P_o at Mach 0.80
47		0.80	1.5	2,340	P_o at Mach 0.80
48	r	0.80	1.5	1,400	P_o at Mach 0.80
49	f	0.23	solid	1,400	Mach No. at med P_o
50	f	0.40	solid	1,400	Mach No. at med P_o
51	f	0.60	solid	1,400	Mach No. at med P_o
52	f	0.70	solid	1,400	Mach No. at med P_o
53	g	1.40	solid	1,400	Mach No. at med P_o
54	h	2.00	solid	1,400	Mach No. at med P_o
55		0.80	0.0 (all taped)	341	Holes
56		0.80	0.0 (5/6 taped)	341	Holes
57		0.80	0.0 (2/3 taped)	341	Holes
58		0.80	0.0 (1/2 taped)	341	Holes
59		0.80	0.0 (1/3 taped)	341	Holes
60		0.80	0.0 (1/6 taped)	341	Holes
61		0.80	0.0	341	Holes

a. run without b. l. rake
b. run with burried transducer in side wall
c. run with accelerometer in side wall
d. run with 1/4 in. spoiler ring
e. run with 1/2 in. spoiler ring
f. solid wall
g. run with 1.4 nozzle
h. run with 2.0 nozzle
r. repeat run

Figure 5. Calibration Test Schedule (Continued)

4.0 FACILITY INSTRUMENTATION

4.1 ACOUSTIC MEASUREMENTS

All fluctuating pressures were detected with quartz transducers manufactured by the Kistler Instrument Corp. They were utilized because they are exceptionally rugged. Included in the data acquisition system were both the acceleration compensated Model #603 transducers and the noncompensated Model #601 transducers. Accelerations were measured with Model #805 accelerometers which were manufactured by the same company. The outputs of all these devices were fed to Kistler Model #504 and #566 charge amplifiers which were remotely grounded. A delay circuit was fabricated that grounded the pressure transducer and accelerometer outputs until 150 milliseconds after the diaphragm burst. This kept the starting transients out of the system. The amplified signals were input to the multiplex system which consisted of a Data Control Systems, Inc., Model GOV-4, voltage controlled oscillator which converted the output to FM. The modulated data traveled through instrumentation cables installed between the MSFC 0.80 m High Reynolds Number Ludwig tube and the instrumentation laboratory located in the main wind tunnel building. There the FM signal was recorded on one of the nine channels of a Consolidated Electrodynamics Corp., Model VR-3600, tape system. Each of the nine channels had a $\pm$20 KC range and a FM separation of 80 KC. After each firing, the data was monitored by transmitting it from the tape system through the demodulator units to a Honeywell Model #1612 Viscorder oscillograph. The data system was calibrated by applying static pressures to the transducers. In addition, a dynamic calibration was carried out with a 1000 Hz signal from a Photocon Research Products, Model PC 125, calibrator.

4.2 DYNAMIC CALIBRATION CONE

Several types of calibration devices that have been used in wind tunnel acoustic evaluations are described in Reference 7. Experience indicates that both pressure transducers mounted on flat surfaces of slender cones and pressure transducers mounted on the test section side walls are a satisfactory means of gathering data.

The ten degree included angle calibration cone is shown in Figure 6. The upper and lower surfaces possess flats for mounting a total of four acoustic pressure transducers. Three acceleration compensated Model #603 transducers and one noncompensated Model #601 transducer were installed on these surfaces. A noncompensated Model #601 transducer was buried in the cone and an accelerometer was also placed in it. Both devices were mounted vertically. Data from two surface mounted Model #603 transducers and from the buried transducer were recorded through 50,000 Hz. Data from the Model #601 transducer were also recorded through this frequency. Data from the remaining Model #603 and from the accelerometers were recorded through 20,000 Hz.

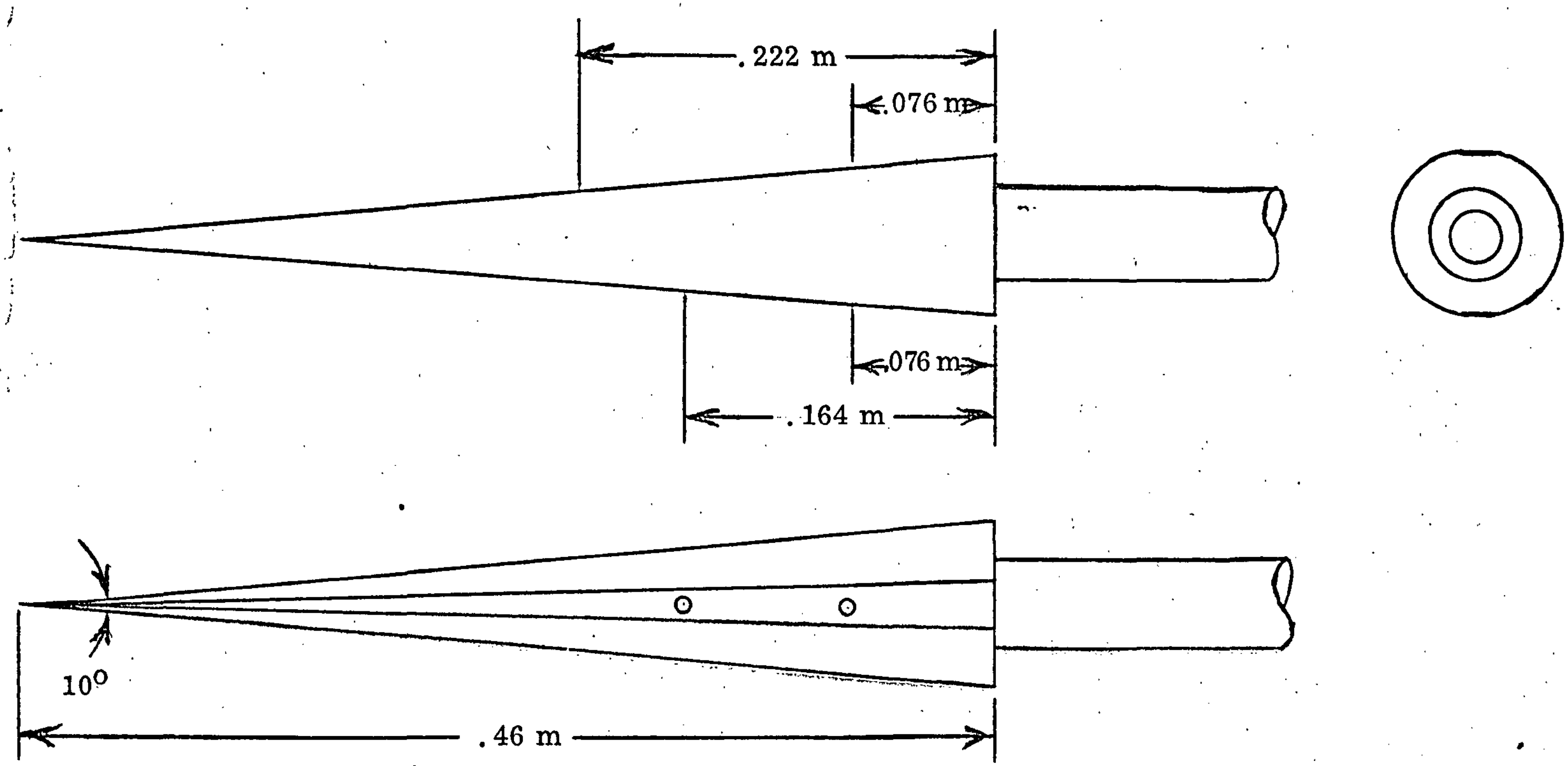

Figure 6. Dynamic Calibration Cone

4.3 WALL DYNAMIC MEASUREMENTS

Data was obtained at the wall of the porous wall test section. Three types of measurements were made. A Kistler Model #603 acceleration compensated transducer was surface mounted. Also at this point, a transducer was buried just below the wall surface. The third measuring device was an accelerometer, mounted at the same place, which measured accelerations in the direction of the pressure transducer axes. The output of each of these sensors was recorded on magnetic tape through 20,000 Hz.

4.4 DATA REDUCTION INSTRUMENTATION

The equipment used in data reduction was similar to that used in the data acquisition. Tapes were played on a Consolidated Electrodynamics Corp., Model VR-3600, tape system through output voltage controlled oscillators. The output was monitored with a Honeywell Model #1612 Viscorder oscillograph. The data was reduced by feeding it in 300 millisecond samples to a Princeton Applied Research, Model 100, correlator. The data was reduced over the entire frequency range of the recording and also over limited frequency bands which were provided by filters. The resulting autocorrelations gave the amplitude and the frequency composition of the noise.

4.5 BOUNDARY LAYER RAKE

A boundary layer rake was designed and fabricated for the facility. The purpose of the device was to measure the thickness of the wall boundary at the aft end of the porous wall test section. The mounted probe is shown in Figure 7. To increase the boundary layer thickness, two annular boundary layer spoiler rings were installed at the forward end of the porous wall test section. They formed 1/4 inch and 1/2 inch steps on the inside of the wall.

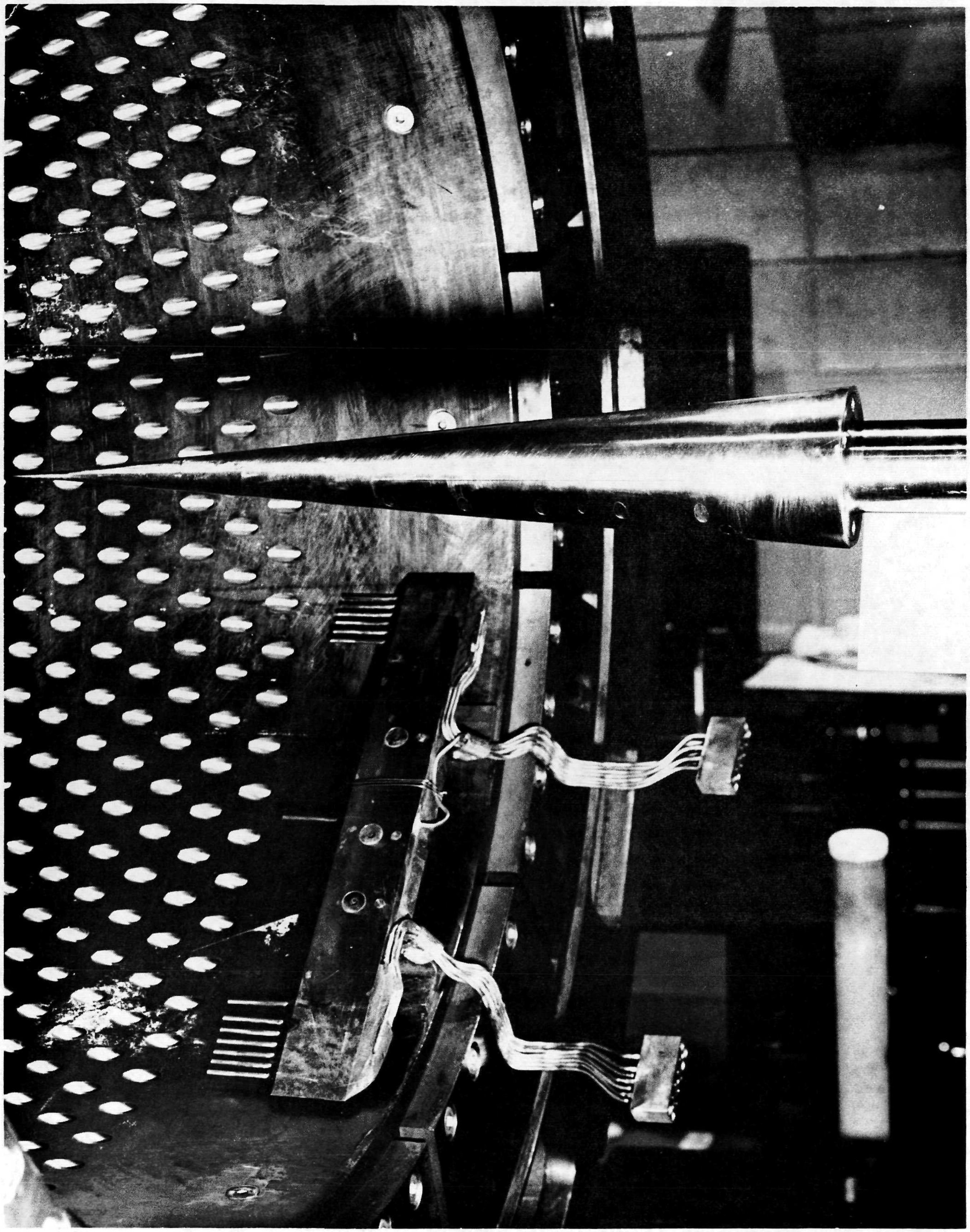

Figure 7. Mounted Calibration Cone and Boundary Layer Rake

5.0 RESULTS OF THE CALIBRATION OF THE MSFC 0.80 M HIGH REYNOLDS NUMBER LUDWIG TUBE

The noise amplitude of this facility is compared in Figure 8 with the amplitudes of other facilities in terms of the fluctuation pressure coefficient, ΔC_p. It is defined as one hundred times the rms value of the acoustic pressure fluctuation, P_{rms}; divided by the dynamic pressure, q. The figure shows a value of $\Delta C_{p\,max} = 5.5\%$ at the center of the test section and $\Delta C_{p\,max} = 7.5\%$ at the wall. These maximum values were obtained at Mach 0.76 with the facility at its minimum operating stagnation pressure of 0.341×10^{-6} M/m^2. These coefficients are slightly in excess of those found in other transonic wind tunnels.

The fluctuation pressure coefficients from the calibration cone are given in Figure 9 as functions of Mach Number. The coefficient is shown at Mach 0.760 for the low stagnation pressure operation and at Mach 0.775 for the maximum operating stagnation pressure of 3.70×10^6 N/m^2. The amplitudes at an intermediate operating stagnation pressure of 1.4×10^6 N/m^2 are also included. The figure shows that the coefficients do not vary greatly with Mach Number. However, the coefficients do decrease by 65% as the stagnation pressure rises from 1.4×10^6 N/m^2 to 3.70×10^6 N/m^2. At these two operating pressures, the absolute amplitudes of the acoustic pressure fluctuations are virtually equal. The reduction in the coefficient is brought about by the increase in dynamic pressure which is caused by the rise in operating stagnation pressure. The fluctuation pressure coefficient, ΔC_p, in this facility at high operating pressure is comparable with those of other wind tunnels.

These test results were obtained by analyzing autocorrelations of noise data. The autocorrelations, which were obtained from 300 millisecond samples, yield noise amplitude and frequency composition. Typical examples are shown in Figure 10. The illustration at the upper left is the autocorrelation of the 1000 Hz calibration signal. The upper right shows the reduced data from a transducer on the calibration cone. The data, filtered below 250 Hz, were obtained at Mach 0.69 with a stagnation pressure of 1.4×10^6 N/m^2 and with test section set at 1.5% porosity. The autocorrelation yields a fluctuation pressure of $\Delta C_p = 5.03\%$ and shows broad-band noise on which a narrow-band disturbance of 2,040 Hz is superimposed.

The effects of variations in porosity are shown in Figure 11. All of this data was obtained on the calibration cone near Mach 0.68 with the stagnation pressure near 1.4×10^6 N/m^2. The overall data was filtered below 250 Hz, and the data illustrating the behavior of the stage II oscillations was filtered below 1,800 Hz and above 3,700 Hz. The figure shows that increasing the porosity from 1.5% to 6.0% decreases the amplitude of the overall fluctuation pressure coefficient by 30%. The figure further illustrates that the amplitude of the stage II porous wall edgetone oscillations is 60% of the overall amplitude. From the preliminary data reduction, the variations in porosity do not cause significant changes in the noise frequency. The noise level in the MSFC 0.80 m High Reynolds Number Ludwig Tube when operating at 6.0% porosity compares favorably with that found in other facilities.

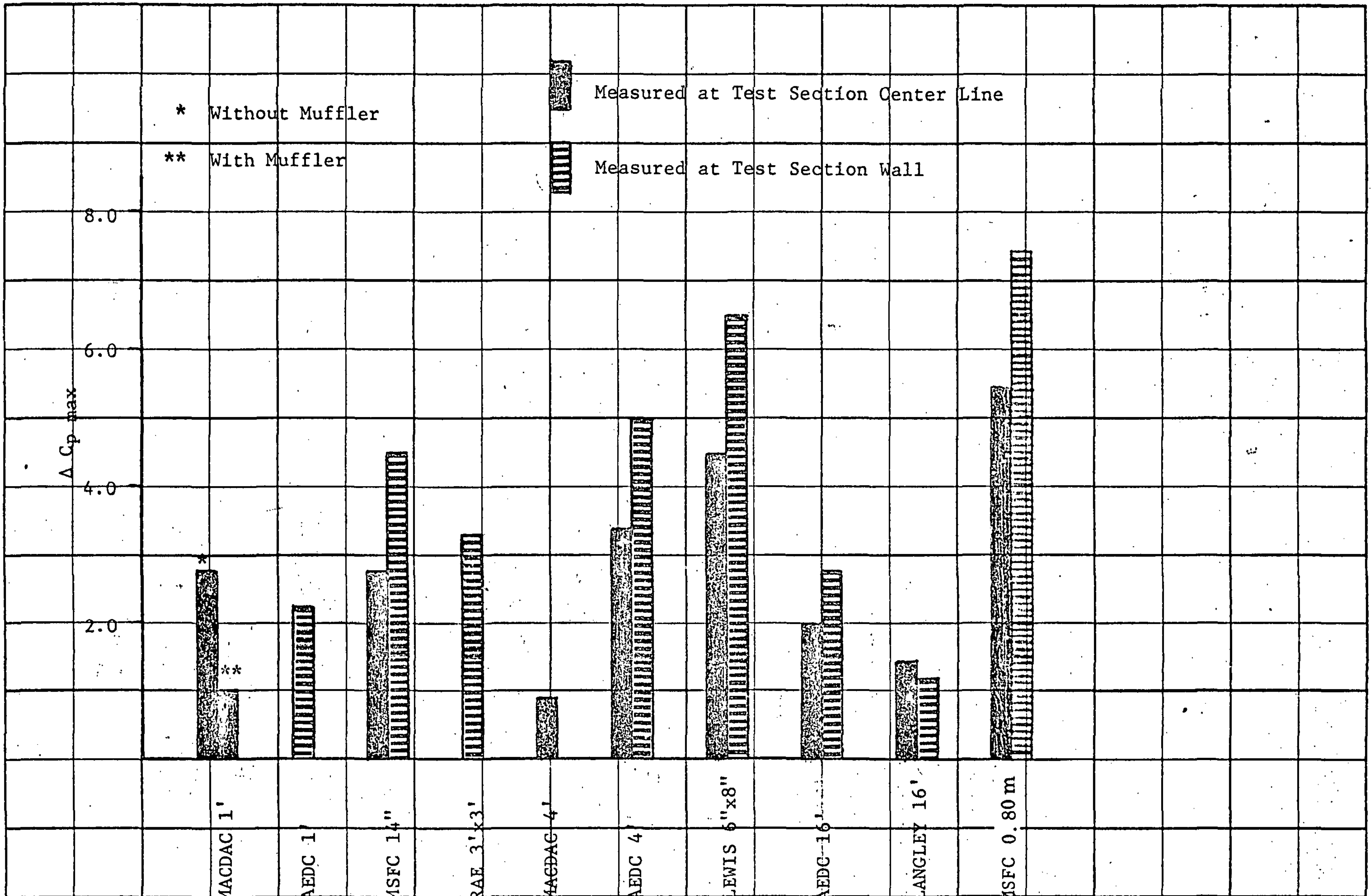

Figure 8. Maximum Fluctuation Pressure Coefficients

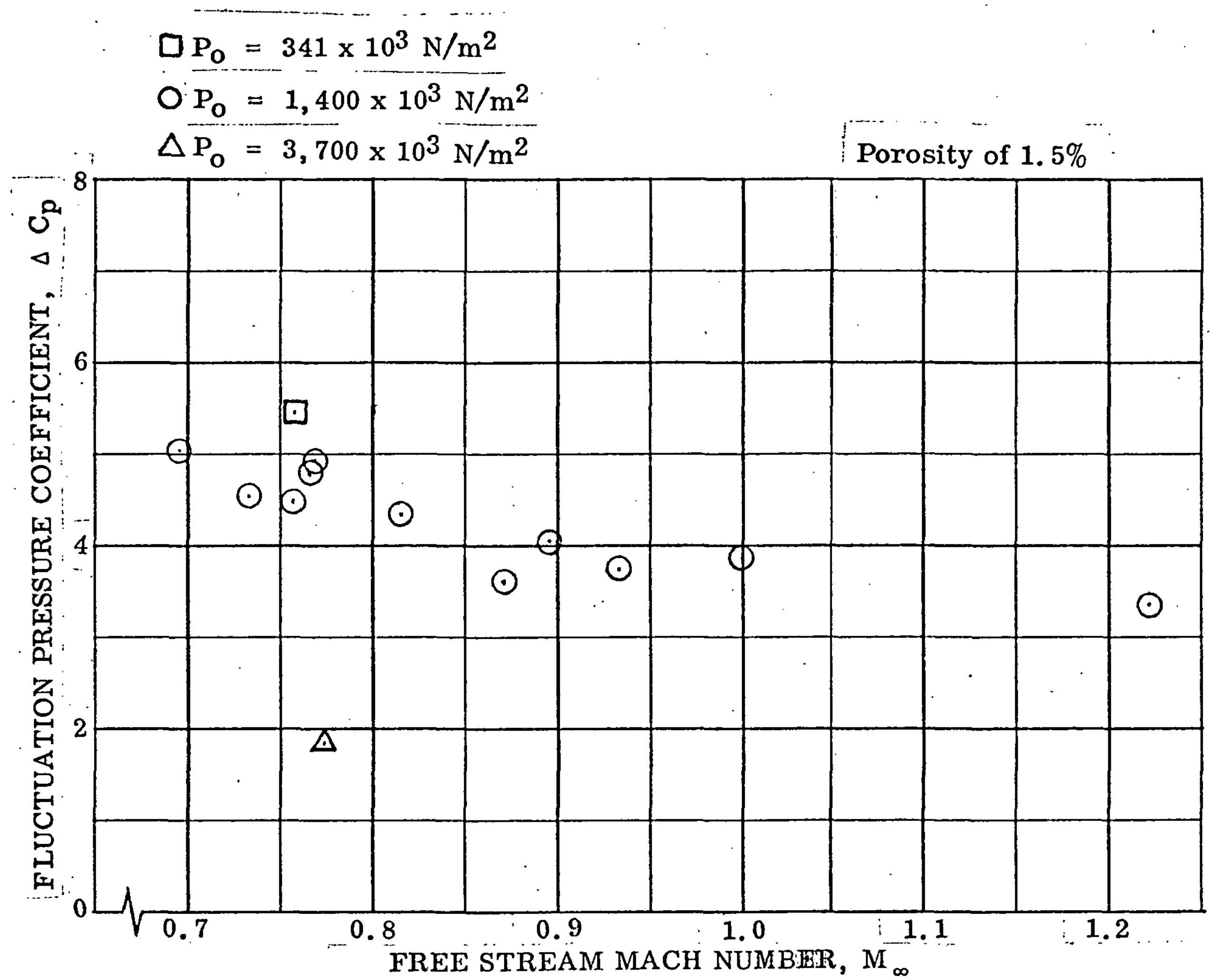

Figure 9. Noise Amplitude In Center of the Test Section

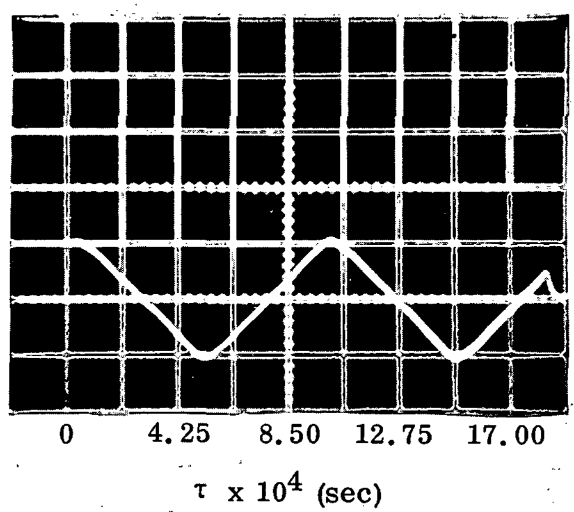

1000 Hz. Calibration Signal

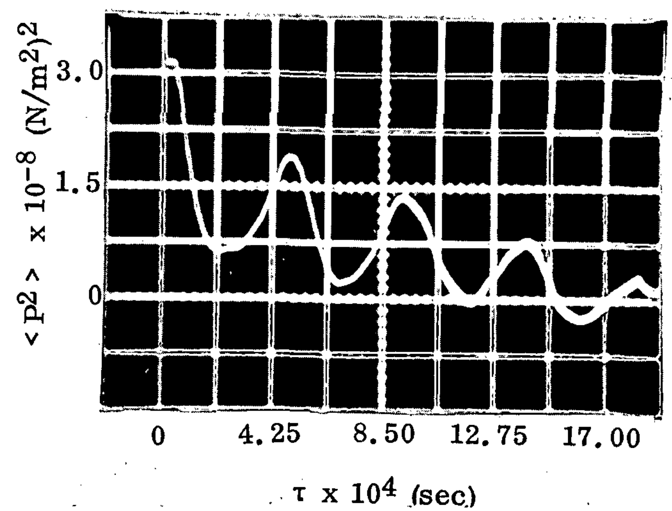

Filtered Below 250 Hz. at 1.5% Porosity

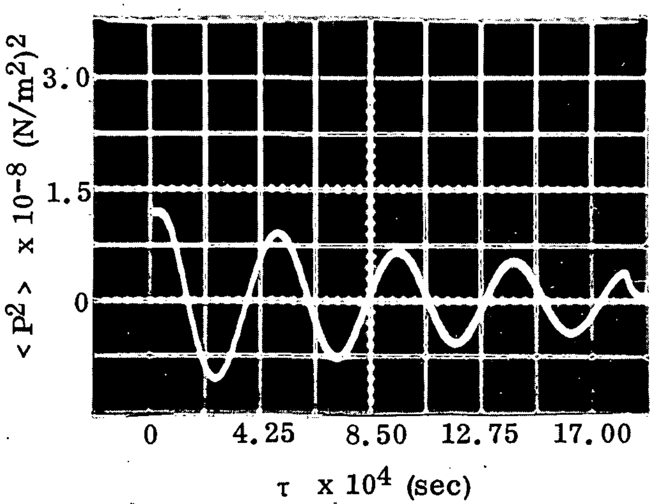

Filtered Below 1,800 Hz and Above 3,700 Hz at 1.5% Porosity

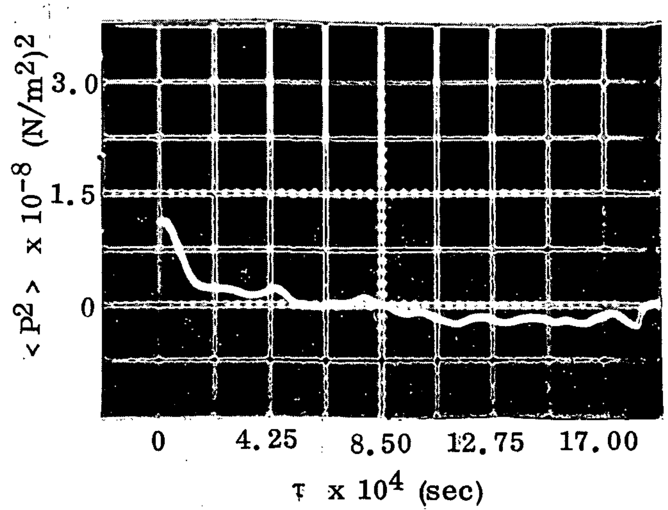

Filtered Below 250 Hz. at 6% Porosity

Figure 10. Autocorrelations

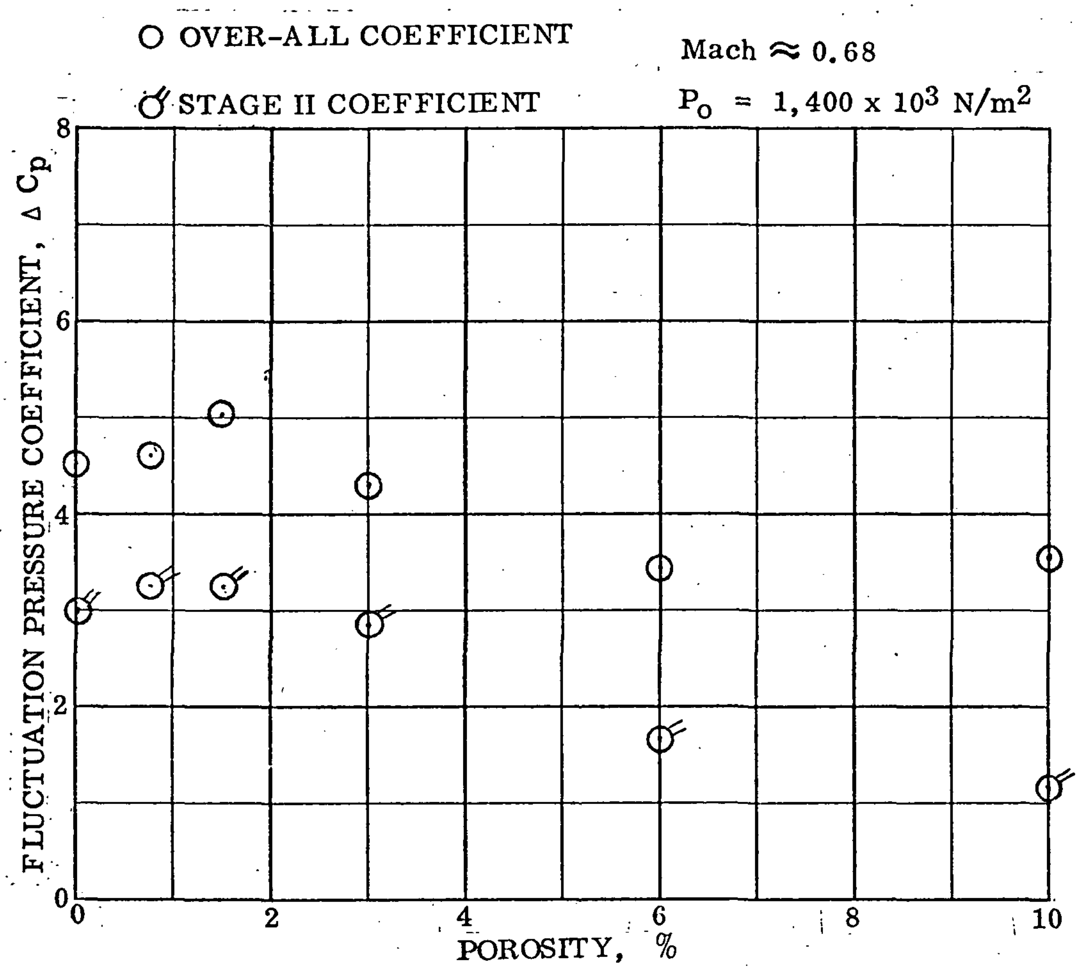

Figure 11. Effects of Variations in Porosity

The autocorrelation shown at the lower left of Figure 10 was derived from the calibration cone. Obtained at Mach 0.68 with a stagnation pressure of 1.4×10^6 N/m^2 and a porosity of 1.5%, the data was filtered below 1,800 Hz and above 3,700 Hz. This illustration shows the stage II narrow-band oscillation at a frequency of 2040 Hz.

The autocorrelation shown at the lower right of this figure was also obtained at Mach 0.68 and a stagnation pressure of 1.4×10^6 N/m^2. However, the porosity was increased to 6.0% and the data was filtered only below 250 Hz. This autocorrelation shows that the porous-wall edgetones virtually disappeared.

The influence of sealing the holes in the porous walls with tape is shown in Figure 12. With a setting of zero porosity, test results were obtained with none of the holes taped, with half of the holes taped, and with all of the holes taped. Because of air leakage at zero porosity, increased Mach numbers occurred with the addition of tape. When none of the holes were taped, Mach 0.75 was recorded. Half of the holes being sealed resulted in Mach 0.85. With all of the holes completely covered, Mach 1.05 was obtained. Taping the holes reduced the overall coefficients by fifty percent and eliminated the porous-wall edgetones.

The frequencies of the narrow-band oscillations from this facility and from seven others are given in Figure 13. The data was normalized to yield approximately (j - 0.5) by the porous-wall edgetone frequency equation which is given in this report as Eq. (1). The frequencies of the disturbances range from 500 Hz in the Lewis 6' x 8' wind tunnel to 20,000 Hz in the MACDAC 4' facility.

Criteria for the occurence of the oscillatory stages in the wind tunnel is suggested by the results of classical edgetone occurrence criteria shown in Figure 14. The critical parameter is the ratio of the jet width to the separation distance between the base of the jet and the tip of the wedge. If this parameter is too large or too small, oscillations of a given stage will not occur. The higher stage oscillations occur at the smaller values of this parameter. Additional discussion of these criteria is given in Reference 5.

Proposed criteria for the occurrence of porous wall edgetone oscillations is based on the ratio of the flat plate displacement boundary layer thickness to the resonant hole separation distance. Figure 15 shows values of this parameter for several wind tunnels. These calculations are made without considering mass removal through the porous walls. The open bars at the right of the figure show the values of the parameter that correspond to the four stages of oscillation. None of the data obtained with the boundary layer rake in the MSFC 0.80 m High Reynolds Number Ludwig Tube has yet been reduced. However, the increase in porosity did decrease the thickness of the boundary layer on the wall, and this diminished boundary layer thickness may have caused the virtual elimination of the porous-wall edgetones.

A summary of the acoustic calibration of eleven transonic wind tunnels is given in Figure 16.

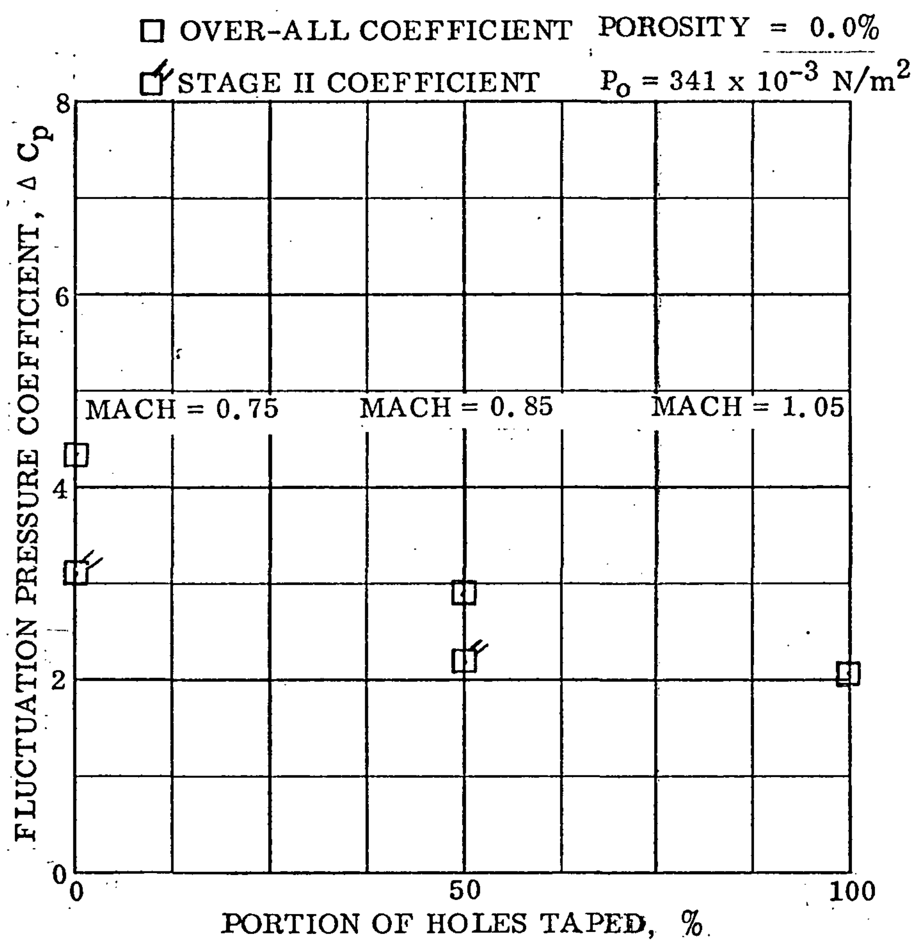

Figure 12. Effect of Taping the Porous-Wall Holes

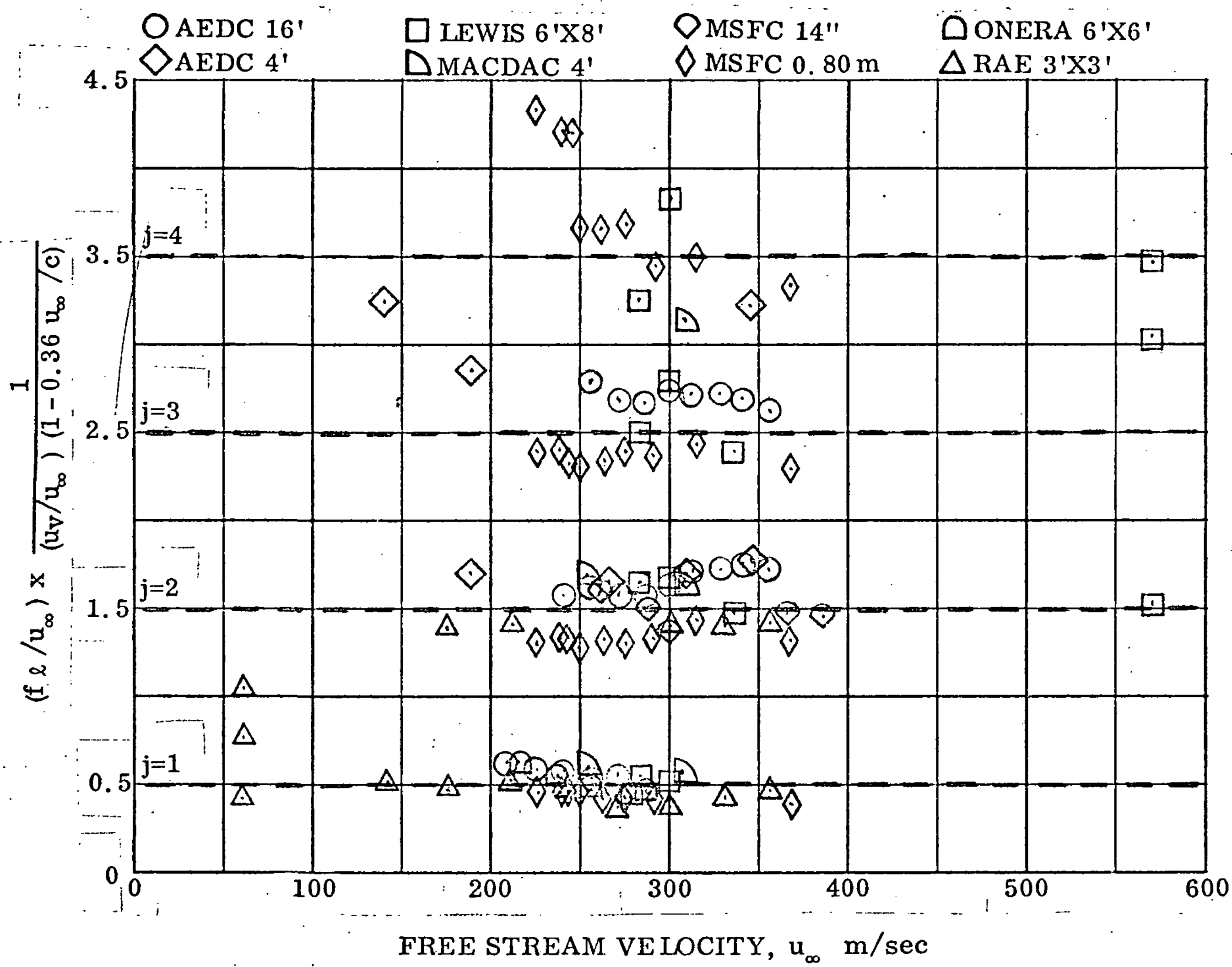

Figure 13. Reduced Frequencies of the Four Porous-Wall Edgetone Stages

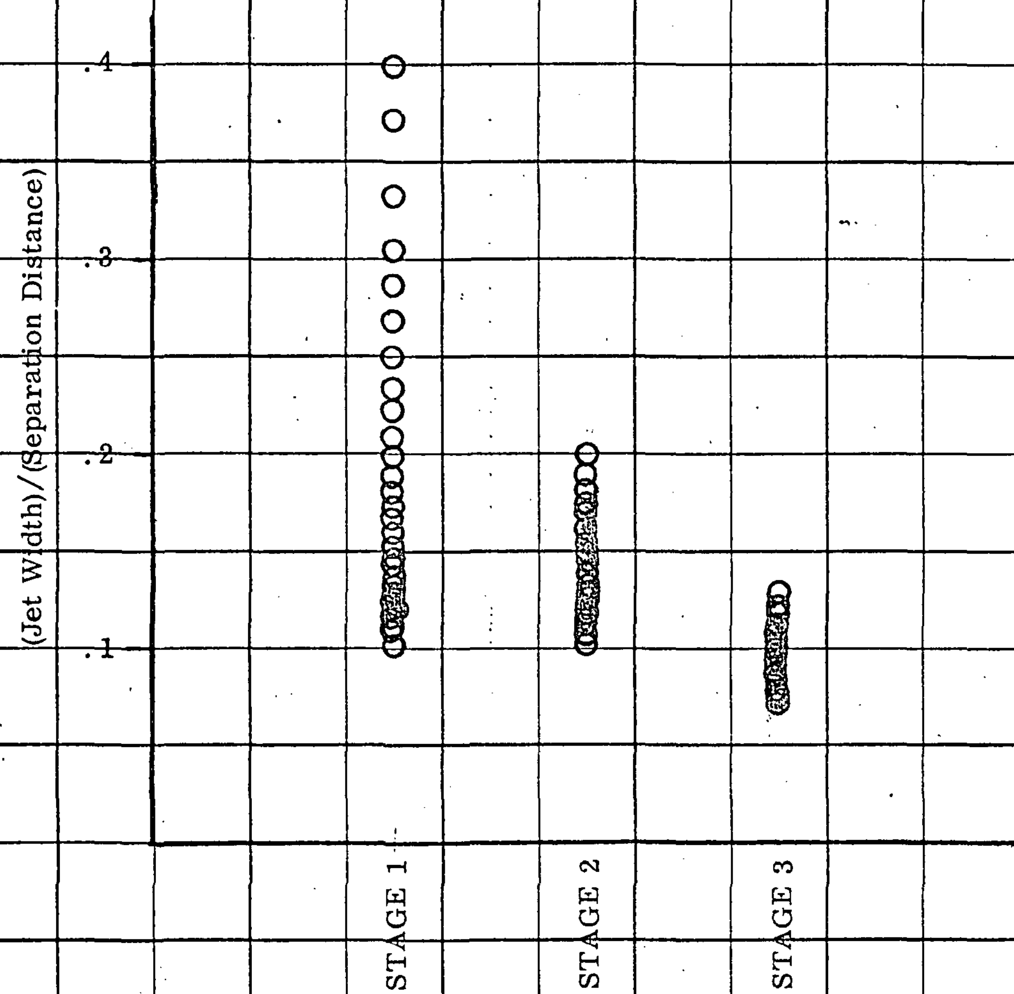

Figure 14. Experimental Range of Classical Edgetone Stages

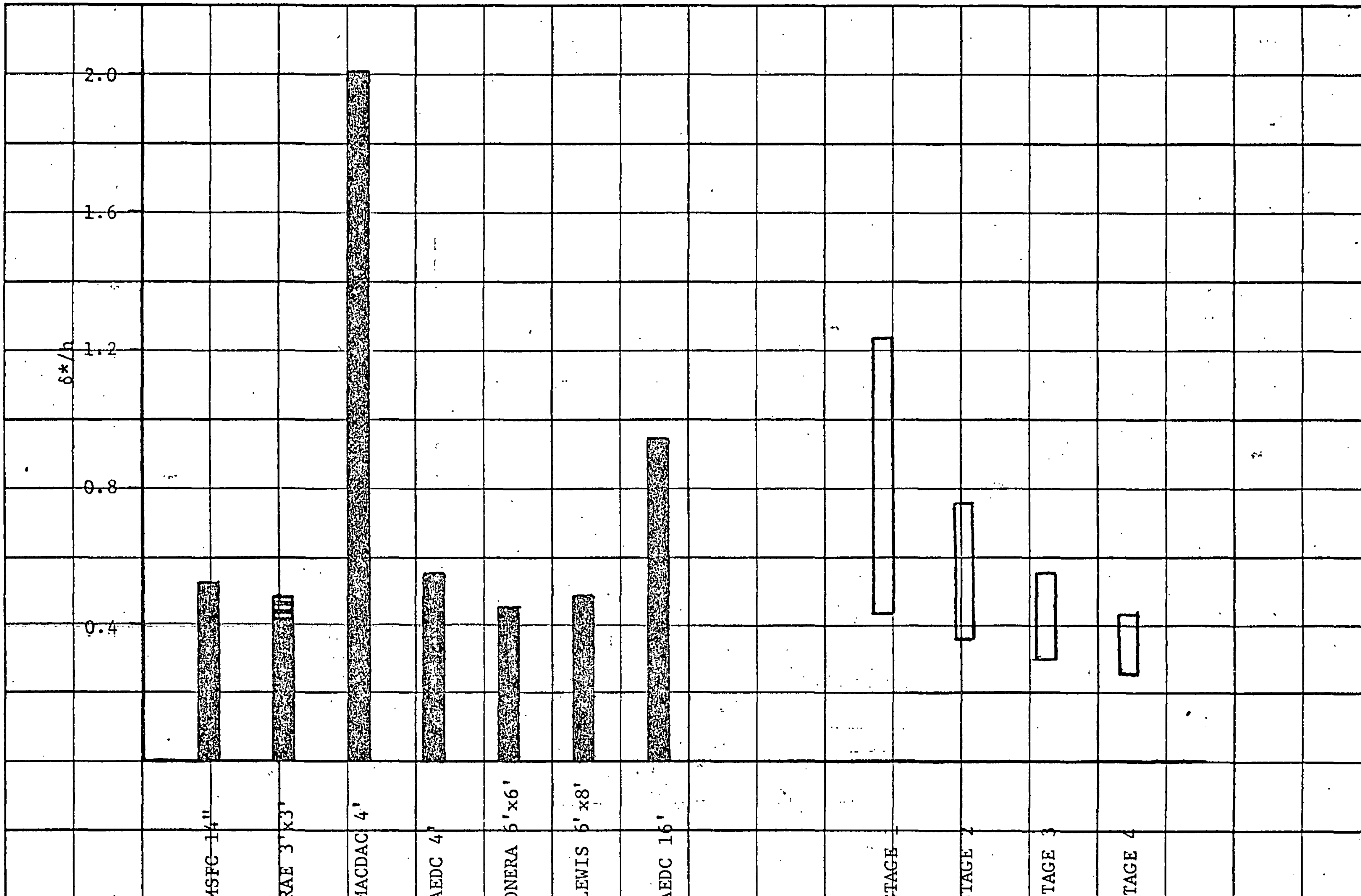

Figure 15. Range of the Ratio of the Flat Plate Displacement Boundary Layer Thickness to Resonant Hole Separation Distance

FACILITY	HOLE DIAMETER (m)	RANGE OF FREQ. (KHz) MEASUREMENT	STAGES DETECTED	RANGE δ^*/h	OUTSIDE DISTURBANCE DETECTED	ΔC_{pmax} AT CENTER LINE	ΔC_{pmax} AT WALL
MACDAC 1'	0.00318(1/8 in)	0+ - 1.0			VALVE JET	2.8 - 1.0	
AEDC 1'	0.00318(1/8 in)	0+ - 1.3			COMPRESSOR		2.2
MSFC 14"	0.00396(5/32 in)	.10 - 20.0	2	0-.527		2.8	4.5
RAE 3'x 3'	0.00952(3/8 in)	0+ - 4.2	1,2	0-.495			3.3
MACDAC 4'	0.00952(3/8 in)	.20 - 100.0	1,2,3	0-2.040		0.9	
AEDC 4'	0.0127(1/2 in)	.03 - 10.0	2,3,4	0-.558		3.4	5.0
ONERA 6'x 6'	0.018(11/16 in)	.05 - 1.1	1	0-.464			
LEWIS 6'x 8'	0.0254(1 in)	0+ - 10.0	1,2,3,4	0-.490	COMPRESSOR	4.5	6.5
AEDC 16'	0.0192(3/4 in)	.03 - 20.0	1,2,3	0-.945		2.0	2.8
LANGLEY 16'	SLOTS	0+ - 20.0				1.4	1.2
MSFC 0.80 m	0.0127(1/2 in)	.25 - 50.0	1,2,3,4			5.4	7.4

Figure 16. Summary of Wind Tunnel Characteristics

REFERENCES

1. G. B. Brown, "On Vortex Motion in Gaseous Jets and the Origin of Their Sensitivity to Sound", Proc. Phys. Soc. 47, Pt. 4, 703-732 (1935).

2. G. B. Brown, "The Vortex Motion Causing Edge Tones", Proc. Phys. Soc. 49, Pt. 5, 493-507 (1937).

3. G. B. Brown, "The Mechanism of Edge-Tone Production", Proc. Phys. Soc. 49, Pt. 5, 508-521 (1937).

4. G. B. Brown, "Jets Musically Inclined", Sci. Progr. (London) 139, 29-51 (1938).

5. G. F. McCanless, Jr., "Additional Correction of 4% Saturn V Protuberance Test Data", Chrysler Corp., Huntsville, Ala. HSM-R1-71 (Jan. 21, 1971).

6. N. Curle, "The Mechanics of Edge-Tones", Proc. Roy. Soc. London, Ser. A, 216, 412-424 (1953).

7. J. R. Boone and G. F. McCanless, Jr., "Evaluation of the Acoustic Sources of Background Noise in Wind Tunnel Facilities," Chrysler Corp., Huntsville, Ala. HSM-R65-68 (June 5, 1968).

TECHNICAL REPORT R5-72

AERONAUTICAL NOISE SUPPRESSION

AT TRANSONIC MACH NUMBERS

By: George F. McCanless, Jr.
George F. McCanless, Jr.

Approved: H. Bader, Jr.
H. Bader, Jr.
Chief Engineer
Engineering Mechanics Department